DOI 10.1007/s10553-024-01690-1
Chemistry and Technology of Fuels and Oils, Vol. 60, No.2, May, 2024 (Russian Original No.2, March– April, 2024)

INNOVATIVE TECHNOLOGIES OF OIL AND GAS

CHARACTERISTIC OF AMPS-BASED SELF-HEALING MATERIAL AND THE EFFECT ON THE PROPERTIES OF OIL WELL CEMENT SLURRY

Lin Zhao[1,2], Haijuan Wang[2], Junhu Yang[2], Lihui Zheng[1] ✉ , Chunyu Wang[3] ✉

The self-healing cement used in oil wells aims to provide long-term interlayer isolation by enabling the cement system to repair itself. This paper compared the absorption properties of 2-acrylamido-2-methyl propanesulfonic acid (AMPS)-based superabsorbent polymer (SAP) and acrylic acid (AA)-based SAP in water and cement slurry filtrate. The effect of cement slurry filtrate on the water absorption properties of the two SAPs was evaluated. The results showed that the calcium ions in the cement slurry would crosslink with the carboxyl groups in the AA-SAP, increasing the crosslink density and greatly reducing its absorption rate in water. Compared to AA-SAP, AMPS-SAP is more suitable for oil well cement slurries. AMPS-SAP can help reduce the fluid loss of cement slurry. The addition of 0.4% AMPS-SAP in cement slurry results in a 64 mL decrease in fluid loss. The properties (rheological properties, thickening time, and compressive strength) of cement slurry meet the requirements for well cementing construction.

Keywords: self-healing cement, superabsorbent polymer, oil well cement, AMPS.

1. Introduction

Cementing is the process of injecting cement slurry into the annular space between the wellbore and casing or between two consecutive casing columns [1, 2]. Once hardened, the cement sheath can support the wellbore and casing, seal the formation, prevent casing corrosion, and control abnormal formation pressure. The primary objective of cementing is to achieve complete and lasting interlayer sealing. However, various factors such as the presence of filter cake, changes in underground temperature and pressure, and volume shrinkage of cement can lead to the development of micro annular gaps at the interfaces [3, 4]. These gaps can form channels for fluid flow in the underground formation. If not repaired promptly, these gaps can compromise the interlayer sealing, leading to fluid channeling.

The self-healing cement [5–7] used in oil wells aims to provide long-term interlayer isolation by enabling the cement system to repair itself. Its greatest advantage is that it enhances the long-term durability of the cement ring without interrupting normal

[1] College of Petroleum Engineering, China University of Petroleum (Beijing), Beijing, China; [2] Petroleum Engineering Technology Research Institute, SINOPEC Henan Oilfield Branch Company, Nanyang, China; [3] College of Materials Science & Engineering, Nanjing Tech University, Nanjing, China. *Corresponding author: Lihui Zheng ✉. E-mail: zhenglihui@cup.edu.cn. Corresponding author: Chunyu Wang ✉. E-mail: wangchunyu@njtech.edu.cn.* Translated from *Khimiya i Tekhnologiya Topliv i Masel*, No. 2, pp. 112–116, March– April, 2024.

oil and gas production. Currently, the main design concept of the self-healing technology involves adding specific materials to the cement slurry [8–13]. Under certain conditions, these materials are activated to generate new substances or provide internal compressive stress to block microcracks. The self-healing material has the ability to sensitively respond to the permeation of oil and gas in microcracks, such as expandable rubber particles. When a cement ring is damaged and produces cracks or micro-gaps, the pre-mixed self-healing material reacts to the stimulation of infiltrating substances by expanding, effectively blocking the oil and gas transport channels. Its advantages include a short response time and significant effectiveness.

In the process of cementing hydrocarbon-rich formations, oil swellable polymers are incorporated into the oil well cement, allowing them to repair microcracks in the cement matrix by swelling in response to the presence of oil or gas [14–18]. When dealing with well cementing that has a high formation water content resulting from long-term water flooding, the use of superabsorbent polymer (SAP) can be effective in preventing fluid channeling, as it has the ability to absorb water and swell [19–21].

In cement concrete, the possibility of incorporating SAP into cementitious materials to increase water content has been investigated by several researchers [22–24]. These cross-linked polymers have the ability to absorb large amounts of liquid and expand significantly to form a soft, insoluble gel. However, their swelling capacity is greatly influenced by the alkalinity and ionic concentration of the solution, resulting in reduced swelling when mixed with fresh concrete. During cement hydration, SAP particles release the absorbed water and contract, creating small macro-pores. Cracks that form are likely to propagate through these pores, and if moisture enters through the crack, the SAP will swell again [20, 24]. If the external fluid has a low ionic concentration, the SAP will expand more than that in the concrete pore solution, causing it to directly block the crack. This physical blocking effect helps prevent further crack propagation. In dry periods, the SAP will release its water content, promoting autogenous healing.

However, the use of SAPs in oil well cement slurry is impeded primarily by their tendency to absorb mixing water, which can hinder pumping. Adding extra water to the slurry is not an option as it diminishes the cement slurry's density, a crucial indicator for cementing operations. Thus, it is crucial to control the water-absorbing capability of SAPs in cement slurry. Furthermore, acrylic acid-based SAPs that are typically utilized in cement concrete lose their water-absorbing capabilities when introduced to oil well cement slurries, primarily because of the influence of calcium ions. When calcium ions interact with carboxyl groups, they create ionic cross-linking that increases the cross-linking density of SAP. This, in turn, leads to a significant reduction in the material's water absorption rate.

In this paper, AMPS, a monomer with minimal influence by calcium ions, was used to prepare the SAP. The absorption properties of AMPS-based SAP and AA-based SAP in water and cement slurry filtrate were compared. The effect of cement slurry filtrate on the water absorption properties of the two SAPs was evaluated. At last, The impact of AMPS-SAP on the properties of cement slurry, including rheological properties, thickening time, fluid loss, and compressive strength, was assessed.

2. Materials and methods

Materials. High sulfate-resistant (HSR) Class G oil well cement was used in this paper. The chemical composition and phase composition (wt.%) of the cement are shown below.

SiO_2 .....21.93
Al_2O_3 .....3.26
Fe_2O_3 .....5.05
TiO_2 .....0.35
CaO 62.33
MgO 1.6
SO_3 .....2.55
K_2O.....0.39
Na_2O.....0.23
MnO 0.1
P_2O_5 .....0.13
LOI.....1.49

C_3S 50.9
C_2S 30.0
C_3A.....1.9
C_4AF.....13.1
Gypsum.....4.1

Monomers N,N-dimethylacrylamide (DMAA, 98%), 2-acrylamido-2-methyl propanesulfonic acid (AMPS, 98%) and acrylic acid (AA, 97%), cross-linking agent methylene-bis-acrylamide (MBA, 99%) and co-initiator N,N,N',N'-Tetramethylethylenediamine (TEMED, 99%) were got from Shanghai Macklin Biochemical Co., Ltd. Sodium hydroxide (NaOH, 95%) and initiator ammonium persulfate (APS, 98%) were got from Sinopharm Chemical Reagent Co., Ltd. Distilled water was used throughout the experiments. Dispersion, fluid loss additive, and retarder were got from commercial sources.

Synthesis of superabsorbent polymers. The superabsorbent polymers (SAPs) were synthesized using an aqueous solution polymerization. Distilled water, monomers, and cross-linking agent (MBA) were sequentially added to the reaction vessel and stirred for 10 minutes until MBA dissolved completely. The solution was then purged with nitrogen to remove any air. Next, the initiator (APS) solution was added gradually, followed by the co-initiator (TEMED) after a 5-minute interval. The solution was stirred for an additional 10 minutes before being allowed to react for 8 hours at 30°C. The resulting product was extracted from the vessel and dried in a vacuum drying oven at 80°C for 24 hours. Finally, the dried product was pulverized and sifted through a 50-mesh sieve to obtain the desired SAPs. AA-SAP was a cross-linked copolymer of DMAA and AA, while AMPS-SAP was a cross-linked copolymer of DMAA and AMPS.

Preparation of cement slurry filtrate. A Cement Slurry Filtrate (CSF) was prepared by conducting a static fluid loss test in accordance with the standard API RP 10B-2: 2013. To create the CSF, 600 g of cement and 264 g of water (with a water-to-cement ratio of 0.44) were thoroughly mixed following the oil well cement slurry preparation procedure. The resulting cement slurry was then poured into an atmospheric consistometer and gradually heated to 60°C at a rate of 3°C/min. Once the atmospheric consistometer reached the target temperature of 60°C, the cement slurry was continuously stirred for an additional 20 min. Subsequently, the cement slurry was transferred to a fluid-loss cell to initiate the filtration of the pore solution, while applying a pressure of 6.9 MPa using nitrogen. The resulting CSF was collected for further testing of its properties in relation to the SAPs.

Water absorption rate. The SAP's water absorption rate is the weight of water absorbed per unit of its own weight. First, a specific amount of SAP powder was weighed and labeled as W_1. Next, the SAP powder was placed in a nylon bag and the combined mass was weighed as W_2. The nylon bag containing the SAP powder was then submerged into a test liquid and periodically removed the bag to absorb any water on its surface using absorbent paper. Finally, the entire mass of the nylon bag and the SAP powder was weighed after water absorption, which was recorded as W_3. Equation was used to calculate the water absorption rate (G, g/g) of the SAP:

$$G = (W_3 - W_2)/W_1. \quad (1)$$

Fourier transform infrared spectroscopy (FTIR). The Bio-Rad FTS135 FTIR spectroscope was utilized to record the FTIR spectra of AMPS-SAP and AA-SAP. To prepare the test sample, the SAP powder and diluent (KBr, spectral pure) were thoroughly ground and then compressed using a tablet press. The wavelength range analyzed was 4000–400 cm^{-1}.

Properties of cement slurry. The properties of cement slurry were carried out according to the API RP 10B-2: 2013, including the rheological property, thickening time, fluid loss, and compressive. The test temperature was set as 60°C.

3. Results and discussion

3.1. Water absorption properties of the SAPs in water and cement slurry filtrate

The absorption rate of AMPS-SAP and AA-SAP was test over time at 60°C in water and in cement slurry filtrate. The second absorption rate of the two SAPs in water after saturated absorption in cement slurry filtrate was also evaluated. The results are shown in **Figure 1**.

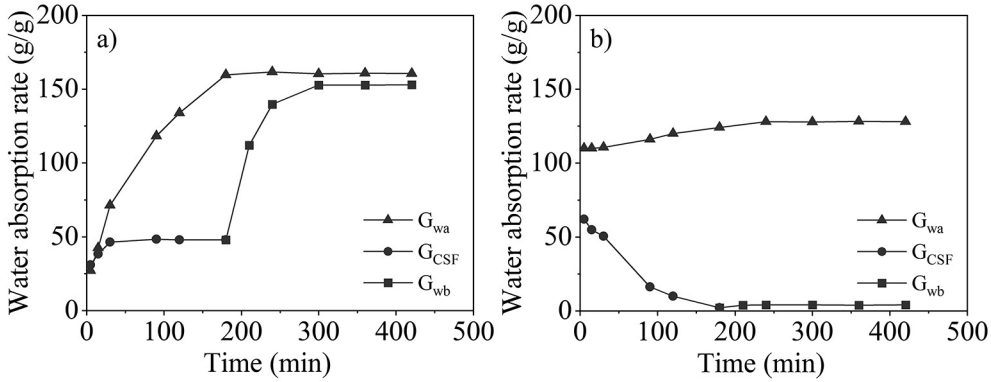

Fig. 1. The absorption rates of the SAPs changed with time in water and in cement slurry filtrate at 60°C; G_{wa} is the absorption rate in water, G_{CSF} is the absorption rate in cement slurry filtrate, and G_{wb} is the second absorption rate in water after saturated absorption in cement slurry filtrate. a) AMPS-SAP; b) AA-SAP

From Fig. 1(a), the absorption rate of AMPS-SAP in water (G_{wa}) increases with time. It reaches saturated water absorption at 180 min, and the saturated water absorption rate is 159.82 g/g. The absorption rate of AMPS-SAP in cement slurry filtrate (G_{CSF}) also increases with time. However, it reaches saturated absorption at 30 min, and the saturated absorption rate is only 48.49 g/g. The presence of ions, specifically calcium ions, in the cement slurry filtrate mainly hinders the water absorption ability of AMPS-SAP. The absorption rate in water is 3.30 times that in cement slurry filtrate. After it is fully saturated with water in the cement slurry filtrate, it was then tested for its second absorption rate in water (G_{wb}). G_{wb} increases with time, and remains essentially unchanged at 300 min. The saturated second water absorption rate is 152.98 g/g, which is not much different from the saturated water absorption rate (G_{wa}). This demonstrates that the presence of ions in the cement slurry does not alter the structure of AMPS-SAP. Consequently, the water absorption performance of AMPS-SAP can be restored when exposed to water with a low ion concentration.

Fig. 1(b) shows the absorption rate of AA-SAP in water and in cement slurry filtrate. It can be found that the absorption speed of AA-SAP in water is extremely rapid, with a capacity to absorb up to 110.09 g/g of water in just 5 min. This accounts for 86.0% of its saturated water absorption rate (128.07 g/g). The absorption speed of AA-SAP in cement slurry filtrate is also fast. It is 62.07 g/g at 5 min. However, it gradually decreases over time. At 180 min, it decreases to 2.19 g/g. At 180 min, the AA-SAP was then tested for its second absorption rate in water (G_{wb}). G_{wb} stabilizes at 4.05 g/g. The water absorption of AA-SAP in cement slurry filtrate is completely different from that of AMPS-SAP. This indicates that the ions in the cement slurry filtrate altered the structure of AA-SAP, reducing the material's water absorption ability.

3.2. FTIR analysis of the SAPs before and after cement slurry filtrate treatment

The AMPS-SAP and AA-SAP were immersed in cement slurry filtrate at 60°C for 180 min. The FTIR spectra of dried samples and untreated samples were tested, as shown in **Figure 2**.

Fig. 2(a) shows the FTIR spectra of AMPS-SAP before and after treatment with cement slurry filtrate. The absorption band at 2933 cm^{-1} is indicative of the unsymmetrical stretching vibrations of aliphatic C–H bonds in methyl groups. The 1544 cm^{-1} band has been identified as the asymmetric stretching of the C=O originating from DMAA and AMPS. The peak at 1044 cm^{-1} corresponds to the C-N-C stretching vibration. The vibrations observed at 1221 cm^{-1} and 1384 cm^{-1} correspond to the symmetric and asymmetric stretching of the (S=O) group, respectively. The FTIR spectra of the samples before and after treatment with cement slurry filtrate showed no changes, indicating that the cement slurry filtrate had almost no effect on the structure of AMPS-SAP.

Fig. 2(b) shows the FTIR spectra of AA-SAP before and after treatment with cement slurry filtrate. The absorption band at 2933 cm^{-1} is indicative of the unsymmetrical stretching vibrations of aliphatic C–H bonds in methyl groups. The 1544 cm^{-1} band has been identified as the asymmetric stretching of the C=O originating from DMAA and AA. The peak at 1044 cm^{-1} corresponds to the C–N–C stretching vibration. The 1716 cm^{-1} band from the sample before treatment with cement slurry filtrate corresponds to the carbonyl stretching vibration of carboxylic acid. However, it disappears at the FTIR spectra of AA-SAP before treatment

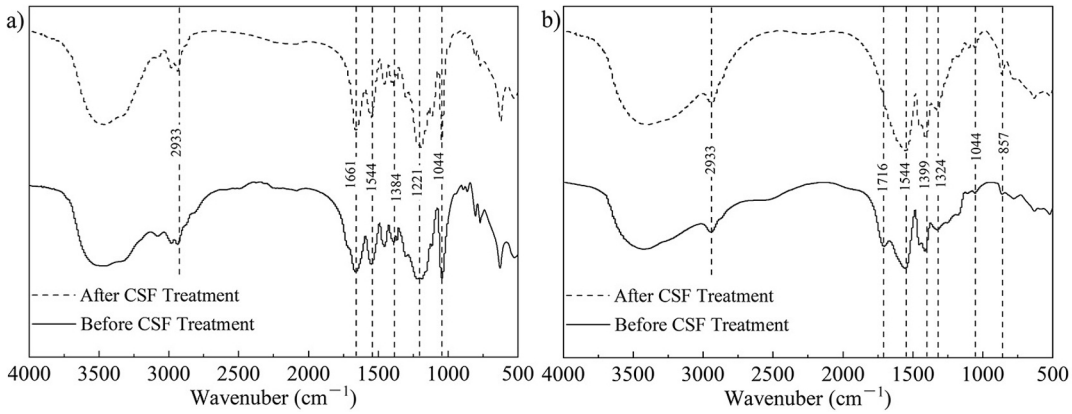

Fig. 2. The FTIR spectra of the SAPs before and after cement slurry filtrate at 60°C for 180 min. a) AMPS-SAP; b) AA-SAP

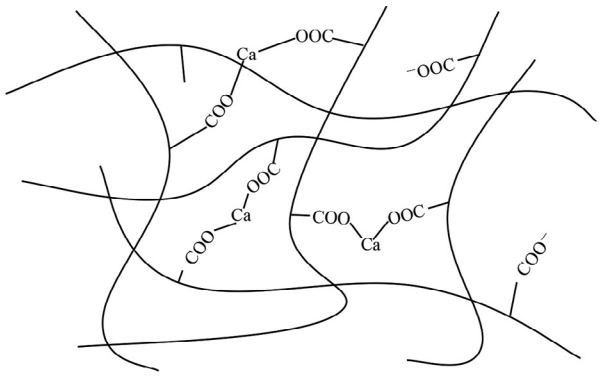

Fig. 3. Schematic diagram of calcium ion cross-linked AA-SAP

with cement slurry filtrate. This indicates that the calcium ions in the cement slurry have cross-linked with the carboxylic acid groups [25–27], thereby enhancing the cross-linking density of SAP and reducing its water absorption capacity.

Figure 3 shows the schematic diagram of the structure of AA-SAP. For AA-SAP not treated with cement slurry filtrate, it is mainly cross-linked by MBA, which contains two C=C bonds. Cross-linking makes SAP form a spatial network structure that can absorb water. As a result, crosslink density affects the water absorption of the SAP. Insufficient cross-link density results in an unstable sap structure that hampers its ability to effectively absorb additional water. Excessive cross-link density hinders the extension of molecular chains during the water absorption process, thereby impeding SAP's ability to absorb water.

AA-SAP molecules contain a significant amount of carboxyl groups, which can undergo ion cross-linking reactions with calcium ions in cement slurry filtrate, thereby increasing the cross-link density of the SAP. As a result, the water absorption rate of SAP in cement slurry filtrate gradually decreases over time, as shown in Fig. 1(b). Furthermore, this ion cross-linking does not dissipate when the solution is replaced with water.

Compared to AA-SAP, AMPS-SAP is more suitable for oil well cement slurries. On one hand, it is unaffected by ion cross-linking in cement slurries, and on the other hand, its water absorption rate in pure water is higher than its absorption rate in cement slurry filtrate. When micro-cracks occur in the cement matrix and water flow is diverted through these cracks, AMPS-SAP is capable of absorbing additional water to seal the cracks.

3.3. Effect of AMPS-SAP on the properties of oil well cement slurry

The impact of AMPS-SAP on the properties of cement slurry, including rheological properties, thickening time, fluid loss, and compressive strength, was assessed. Considering that AMPS-SAP can absorb water from cement slurry and affect its rheological properties, efficient polycarboxylate-based dispersant are applied. The cement slurry formulations are shown in **Table 1**. The test temperature is set as 60°C.

Table 1. Cement slurry formulations

Notion	Cement, g	Water, g	Dispersant, g	Fluid loss additive, g	AMPS-SAP, g
CS0	600	264	3	9	0
CS2	600	264	3	9	1.2
CS4	600	264	3	9	2.4

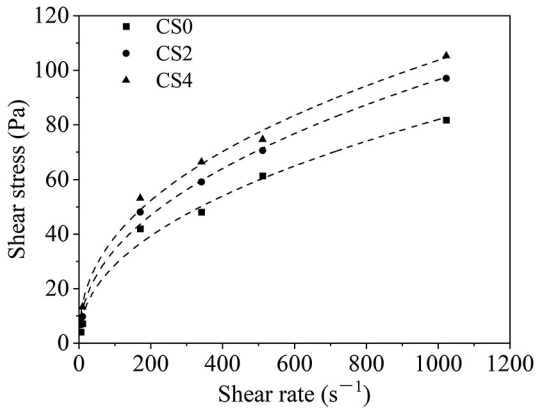

Fig. 4. Rheological curves of the cement slurries at 60°C

Figure 4 shows the rheological curves of the cement slurries at 60°C. It can be found that the shear stress of cement slurry increases with the increase of AMPS-SAP dosage at the same shear rate. The rheological pattern of cement slurries are that of Power-law fluid. The rheological curves of cement slurries were fitted using Eq. (2), and the corresponding results are presented in **Table 2**. All the cement slurries exhibit a flow behavior index (n) that is less than 1, suggesting that they are pseudoplastic fluids (i.e., shear thinning fluids). Additionally, the consistency index (k) of a cement slurry is directly proportional to its effective viscosity and related to the cohesion of individual particles. consistency index (k) is gradually increases with the increase of AMPS-SAP dosage. This indicates that the absorption of water by AMPS-SAP increases the viscosity of cement slurry. However, the rheological properties of cement slurry with 0.4% SAP addition still meet the requirements for well cementing.

$$\tau = k \cdot \gamma^n, \tag{2}$$

where τ is Shear force, Pa; γ is Shear rate, s^{-1}; k is Consistency coefficient, $Pa \cdot s^n$; n is Flow behavior index, dimensionless.

The effect of AMPS-SAP on the thickening time of cement slurry is shown in **Figure 5**. The initial consistency of cement slurry is minimally affected by AMPS-SAP, and the initial consistency of the three cement slurries is about 20 Bc. However, the thickening time of cement slurry increases with the increase of AMPS-SAP dosage. Compared to CS0, the addition of 0.2% AMPS-SAP in CS2 results in a 16-minute increase in the thickening time, while the thickening time of CS4, which contains 0.4% AMPS-SAP, is prolonged by 21 min. This is mainly because the uncrosslinked molecular chains in AMPS-SAP dissolve in the cement slurry, delaying the hydration of cement.

The fluid loss of the three cement slurries: CS0 – 106 mL, CS2 – 73 mL, CS4– 42 mL.

AMPS-SAP can help reduce the fluid loss of cement slurry. Compared to CS0, the fluid loss of CS2 decreases by 33 mL, while the water loss of CS4 decreases by 64 mL. The monomers used to prepare AMPS-SAP in this paper is also the main monomers used to prepare commonly used AMPS-based fluid loss additive [28–30]. On the one hand, it may be that the uncrosslinked

Table 2 Fitting results of rheological curves of the cement slurries

Notion	Rheological model	Fitting function	R^2	n	k ($Pa \cdot s^n$)
CS0	Power-law fluid	$\tau = 3.51\gamma^{0.56}$	0.985	0.56	3.51
CS2	Power-law fluid	$\tau = 4.37\gamma^{0.45}$	0.993	0.45	4.37
CS4	Power-law fluid	$\tau = 5.51\gamma^{0.42}$	0.993	0.42	5.51

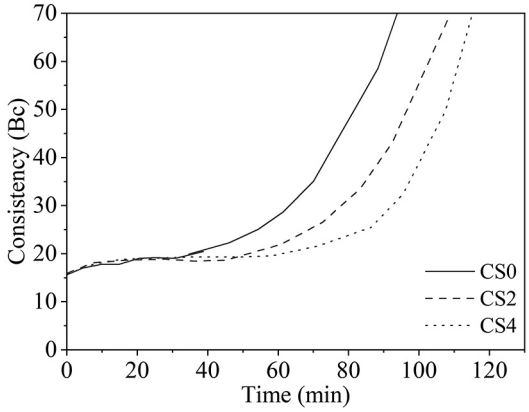

Fig. 5. Thickening curves of the cement slurries at 60°C

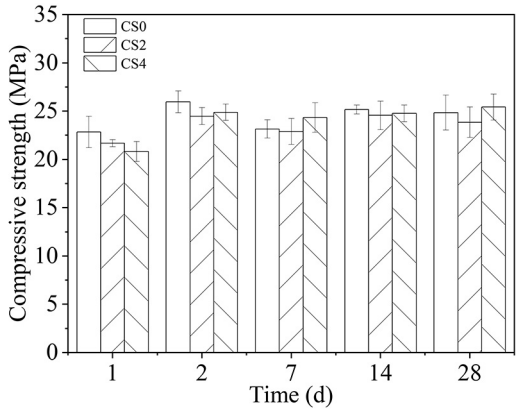

Fig. 6. Compressive strength of cement matrix at 60°C

segments adsorb on the surface of cement particles and reduce fluid loss. On the other hand, it may be that the AMPS-SAP after water absorption fills the pores of the filter cake.

The effect of AMPS-SAP on the compressive strength of cement matrix is shown in **Figure 6**. According to Fig. 6, it can be observed that the addition of AMPS-SAP has a minor effect on the compressive strength of cement matrix. At 1 d, the maximum influence of AMPS-SAP on the compressive strength of cement matrix is observed, with compressive strengths of 20.69 MPa and 20.81 MPa for CS2 and CS4 cement matrix, respectively, representing a reduction of 5.08% and 8.93% compared to CS0. Within 28 d, the compressive strength of cement matrix with different dosages of AMPS-SAP remains above 14 MPa (meeting the basic requirements for compressive strength in cementing construction).

4. Conclusions

The saturated absorption rate of AMPS-SAP in water is 159.82 g/g, while the saturated absorption rate of AMPS-SAP in cement slurry filtrate is 48.49 g/g. Cement slurry filtrate has little effect on the absorption ability of AMPS-SAP in water. However, cement slurry filtrate reduces the absorption rate of AA-SAP in water. FTIR spectra indicates that the calcium ions in the cement slurry have cross-linked with the carboxylic acid groups, thereby enhancing the cross-linking density of AA-SAP and reducing its water absorption capacity. AMPS-SAP can help reduce the fluid loss of cement slurry. The addition of 0.4% AMPS-SAP in CS4 results in a 64 mL decrease in fluid loss. The properties (rheological properties, thickening time, and compressive strength) of cement slurry meet the requirements for well cementing construction.

REFERENCES

1. C. Wang, L. Wang, X. Yao, et al. The effect of rutin on the early-age hydration of oil well cement at varying temperatures. Cem. Concr. Compos. **128**, 104438 (2022).

2. S. Guo, Y. Bu, A. Zhou, et al. A three components thixotropic agent to enhance the thixotropic property of natural gas well cement at high temperatures. J. Nat. Gas Sci. Eng. **84**, 103699 (2020).

3. Y. Liu, T.A. Tong, E. Ozbayoglu, M. Yu, E. Upchurch, An improved drift-flux correlation for gas-liquid two-phase flow in horizontal and vertical upward inclined wells. J. Pet. Sci. Eng. **195**, 107881 (2020).

4. Y. Liu, E.R. Upchurch, E.M. Ozbayoglu, Experimental study of single taylor bubble rising in stagnant and downward flowing non-newtonian fluids in inclined pipes. Energies **14**(3), 578 (2021).

5. P.H. Cavanagh, C.R. Johnson, L. Roy-Delage, et al. SPE/IADC Drilling Conference (2007).

6. R.P. Darbe, J. Karcher, K. Pewitt, in Middle East Drilling Technology Conference & Exhibition (2009). h

7. C. Wang, Y. Bu, S. Guo, Y. Lu, et al. Self-healing cement composite: Amine- and ammonium-based ph-sensitive superabsorbent polymers. Cem. Concr. Compos. **96**, 154–162 (2019).

8. L. Lv, Z. Yang, G. Chen, G. Zhu, et al. Synthesis and characterization of a new polymeric microcapsule and feasibility investigation in self-healing cementitious materials. Constr. Build. Mater. **105**, 487–495 (2016).

9. Z. Peng, C. Yu, Q. Feng, et al. Preparation and application of microcapsule containing sodium potassium tartrate for self-healing of cement. Energ. Source. Part A **45**(2), 1–13 (2019).

10. D. Sun, M. Wenxu, M. Jikun, et al. Wang, The synthesis of dmtda microcapsules and investigation of self-healing cement paste through an isocyanate-amine system. Cem. Concr. Compos. **122**, 104132 (2021).

11. G. Souradeep, H.W. Kua, Encapsulation technology and techniques in self-healing concrete. J. Mater. Civ. Eng. **28**(12), 04016165 (2016).

12. W. Mao, C. Litina, A. Al-Tabbaa, Development and application of novel sodiumsilicate microcapsule-based self-healing oil well cement. Materials **13**(2), 456 (2020).

13. S. Papaioannou, M. Amenta, V. Kilikoglou, et al. Synthesis and integration of cement-based capsules modified with sodium silicate for developing self-healing cements. Constr. Build. Mater. **316**, 125803 (2022).

14. Z. Lu, X. Kong, R. Yang, et al. Oil swellable polymer modified cement paste: Expansion and crack healing upon oil absorption. Constr. Build. Mater. **114**, 98–108 (2016).

15. R. Zhang, X. Mao, Z. Zhao. Synthesis of oil-swelling material and evaluation of its self-healing effect in cement paste. Polyme-Plast. Tech. Mat. **58**(6), 618–629 (2019).

16. C. Johnson, A. Gai, T. Ioan, et al. IPTC International Petroleum Technology Conference (2019). https://doi.org/ 10.2523/ IPTC-19399-MS

17. C. Wang, Y. Bu, L. Zhao. Properties and self-healing behavior of oil absorbent microspheres modified cement. Smart Mater. Struct. **26**(9), 095010 (2017).

18. S. Nafikova, A. Bugrayev, S. Taoutaou, et al. SPE Annual Technical Conference and Exhibition (2019).https://doi.org/10.2118/195945-MS

19. H. Liu, Y. Bu, J.G. Sanjayan, et al. The application of coated superabsorbent polymer in well cement for plugging the microcrack. Constr. Build. Mater. **104**, 72–84 (2016).

20. L. Zhao, N. Li, J. Yang, et al. Alkali-resistant and ph-sensitive water absorbent self-healing materials suitable for oil well cement. Energies **15**(20), 7630 (2022).

21. L. Zhao, L. Zheng, Y. Liu, et al. AADE National Technical Conference and Exhibition (2023)

22. D. Snoeck, S. Steuperaert, K. Van Tittelboom, et al. Visualization of water penetration in cementitious materials with superabsorbent polymers by means of neutron radiography. Cem. Concr. Res. **42**(8), 1113– 1121 (2012).

23. D. Snoeck, K. Van Tittelboom, S. Steuperaert, et al. Self-healing cementitious materials by the combination of microfibres and superabsorbent polymers. J. Intell. Mater. Syst. Struct. **25**(1), 13–24 (2014).

24. H. Lee, H. Wong, N. Buenfeld, Potential of superabsorbent polymer for self-sealing cracks in concrete. Adv. Appl. Ceram. **109**(5), 296–302 (2010).

25. J. Yu, Y. Wang, Y. He, et al. Calcium ion-sodium alginate double cross-linked graphene oxide nanofiltration membrane with enhanced stability for efficient separation of dyes. Sep. Purif. Technol. **276**, 119348 (2021).

26. B. Yan, X. Hu, Y. Zhao, et al. Research and development of a sodium alginate/calcium ion gel based on in situ cross-linked double-network for controlling spontaneous combustion of coal. Fuel **322**, 124260 (2022).

27. Z. Li, J. Guo, F. Guan, et al. Oxidized sodium alginate cross-linked calcium alginate/antarctic krill protein composite fiber for improving strength and water resistance. Colloids Surf. A **656**, 130317 (2023).

28. J. Plank, A. Brandl, Y. Zhai, et al. Adsorption behavior and effectiveness of poly (n, n-dimethylacrylamide-co-ca 2-acrylamido-2-methylpropanesulfonate) as cement fluid loss additive in the presence of acetone-formaldehyde-sulfite dispersant. J. Appl. Polym. Sci. **102**(5), 4341–4347 (2006).

29. J. Plank, A. Brandl, N.R. Lummer, Effect of different anchor groups on adsorption behavior and effectiveness of poly (n, n-dimethylacrylamide-co-ca 2-acrylamido-2-methylpropanesulfonate) as cement fluid loss additive in presence of acetone–formaldehyde–sulfite dispersant. J. Appl. Polym. Sci. **106**(6), 3889–3894 (2007).

30. C. Tiemeyer, J. Plank, Working mechanism of a high temperature (200°C) synthetic cement retarder and its interaction with an AMPS®-based fluid loss polymer in oil well cement. J. Appl. Polym. Sci. **124**(6), 4772–4781 (2012).